ASTRON 120 Lab 2 Report - Introduction to Spectroscopy

Quentin Le Ny
UC Berkeley
Department of Astronomy
quentin.le.ny@berkeley.edu
Group 4A
Quentin Le Ny, Maxwell Coy, Cole Trudgen

October 8, 2024

Abstract

The lab results discussed in this report focus on spectrographic measurements taken of the Sun, and of surrounding physical features for comparison of spectra. In astronomy, understanding spectral lines and the role they play in identifying the composition of stellar, planetary, and other extra-terrestrial objects is crucial. It allows scientists to deduce further information about the observed object, adding to our understanding of the universe and its contents. To build and calibrate a spectrograph, it will be necessary to first construct a system including an imager, optical lens, diffractor, collimator, and a light source. By analyzing the light emitted from an assortment of gas discharge lamps, it is possible to perform calibration. This can be verified by checking the angle of dispersion of the spectrograph, measured to be $-0.19°$, which gave us a spectral resolution of 177 at the center of our images. Once these crucial steps are completed, the accuracy of observations of the Sun's spectrum is ensured. This will allow for the extraction of spectral lines, using them to examine the absorption lines of the Sun, and of a random cloud in the sky. It is then possible to visualize how the fluxes of these two objects vary over a wavelength range by computing the ratio of these spectra, plotting it over a wavelength range. The expected result, achieved in most part by the process described in this report, is that according to a power law balancing the orders of magnitude of the two fluxes, the slope of the flux ratio versus wavelength remains linear.

Nomenclature

- spectrograph/spectroscopy
- light spectrum/spectral lines
- collimator
- diffractor
- incidence angle
- angular dispersion
- spectral resolution
- linear least squares fitting

1 Introduction

The most crucial part of this experiment is arguably in ensuring the calibration of a spectrograph, allowing for an accurate observation of the Sun's spectral lines, which can then indicate what the possible composition of the Sun's spectra is. An important note to make at this point is that the spectrograph used to procure the results in this report had to be realigned shortly before the capturing of final results. Resultantly, the amount of gas lamps

used for calibration were minimal, so it's possible that the errors in the final results are wider than they would have been in an optimal situation. Regardless, spectral pictures of all the different gas lamps (Hydrogen, Oxygen, Water, Nitrogen, Neon) were taken, and subsequently uploaded for conversion via programming functions using Python in Google Colaboratory. For this report, the element of choice for calibration will be Neon (specifically, Ne I lines). Alongside the capturing of the various spectral signatures, flat and dark frames were taken for image cleaning. The cleaned images were then ran through some more coded programs to identify the strong emission lines in the gas' spectra, which were then noted down according to their pixel location on the x-axis. This will be covered in Section 2.1 of this report. Section 2.2 then details the analysis performed to convert the pixel locations of these lines to wavelength values. This conversion was initialized by obtaining accurate experimental values of strong emission wavelength lines for Neon from the Basic Atomic Spectroscopic Data section of the National Institute of Standards and Technology's (NIST) website [1]. These values were then fitted to a polynomial, correlating the true neon wavelength values to the recorded neon line pixel locations, using the method of linear least squares. The equation for this fit is defined as such:

$$\hat{\beta} = \arg\min_{\beta} \left(\sum_{i=1}^{n} \frac{(y_i - p(x_i, \beta))^2}{\sigma_i^2} \right)$$

This will allow us to map out the entire spectrum for each gas according to pixel locations of suspected strong emission lines, enabling us to move on to determining the spectral resolution and wavelength range of our spectrograph. The wavelength range can be taken by finding the difference between the strong line with the smallest pixel location value and the biggest.

$$\Delta\lambda = \lambda_{\text{sl, max}} - \lambda_{\text{sl, min}}$$

This value can then be plugged into the following equation to find the spectral resolution at a certain wavelength:

$$R = 1000 \left(\frac{f_1 \left(\sin(\text{rad}(\theta_I)) + \sin(\text{rad}(\theta_D)) \right)}{l_s \cos(\text{rad}(\theta_D))} \right)$$

Descriptions for each of the variables can be found in the Appendix of this report. Now, with these calculations out of the way, the final section of this report can be moved onto, which covers the process to visualize the elemental composition of the Sun's spectra. Finally, comparing the images of the sunlight to other objects in the sky, we can characterize the change of spectral slope between different sources of outdoor light.

2 Spectrograph Calibration

This section will highlight the work done on calibrating the spectrograph - this includes observing and plotting spectra of several lamps (incandescent and gas discharge), comparing those results with accurately known spectra of said lamps, as well as assessing the spectral resolution and wavelength range of the imager.

The components of the spectrograph include:

- Blackfly Monochrome BFS-PGE-19S4C: 1,616 x 1,240 pixels, pixel size: 4.5 μm
- Optical Lens: AC254-075-A, Ø=25.4mm, F=75.0mm, Visible Achromat
- Collimator (F=50.0mm)
- Diffractor
- Slit for light directioning (100micron width)

The materials allowing the recording of observations include:

- Light source: LED (?) + Power supply
- Notecards, tape, rulers, cardboard, jacket
- Posts, post holders, post holder bases
- Optical system breadboard
- Optical telescope (Cassegrain)

The spectrograph's components, were placed on an optical system breadboard, arranged as in the diagram below.

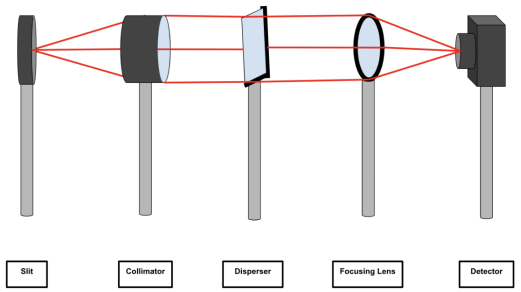

Figure 1: System Design

2.1 Observing and Plotting Spectra of Light Sources

To begin the calibration of the spectrogram, we needed multiple light sources, originating from light emission of a bulb, each containing a different element. The elements from which a light signature was obtained are as follows: $\{N_2, O_2, H_2, H_2O, Ne\}$.

Since time only allowed for a full-depth analysis of one element, Neon was selected as the element of choice.

After an imaging cleaning of the Neon readings, we plotted a color map of the image, where brighter colors indicate the strength of emissions from the Neon gas. Our image (Figure 2) shows multiple discrete ellipses, separated by different lengths. Their centers indicate the strong emission lines, which we marked with vertical lines, shown in Figure 3.

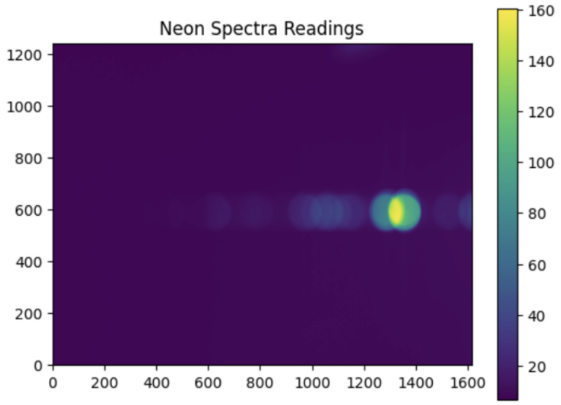

Figure 2: Neon Spectra Readings

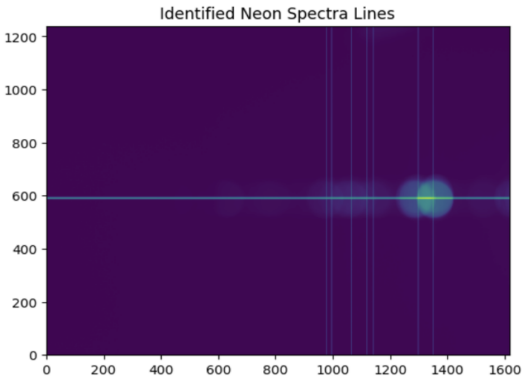

Figure 3: Identified Neon Spectra Lines over Reading

To help visualize these strong lines better, and to check for any excessive variations from the strong lines that we may have missed in our analysis, we plotted the data points and their pixel location ranges, shown in Figure 4.

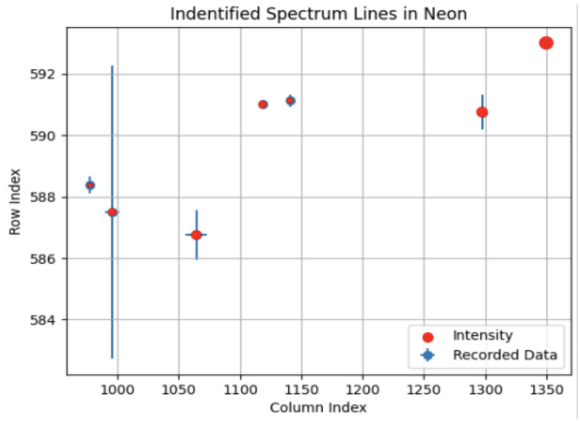

Figure 4: Graph of Identified Spectra Lines in Neon

2.2 Conversion of Spectra by Pixel Size to Wavelength

Now that we knew what the relative spacing was between the seven strong emission lines we identified, we compared them to data from the NIST[1]. The two plots below (Figures 6 and 7) represents the recorded pixel locations and true wavelengths, for Neon, respectively. Figure 7 only shows strong emission lines for the visible light range, as indicated by the color coding of the lines.

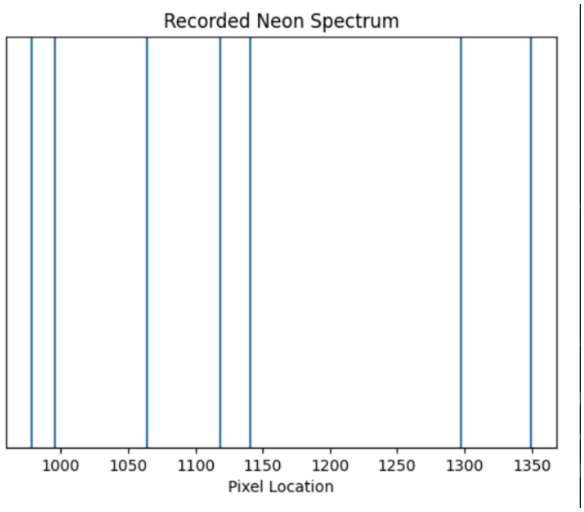

Figure 5: Recorded Neon Spectrum Pixel Locations

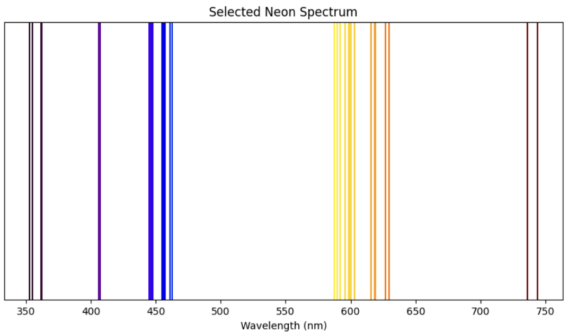

Figure 6: True Neon Spectrum in Visible Light Range

In order to approximate a correlation between these two data sets, we chose 7 wavelengths that visually appeared to have a similar pattern of spacing compared to the recorded pixel locations, and plotted them. We then fit a polynomial of first degree, using the linear least squares method described in the introduction. This returned the graph below, which shows a positive, moderately linear correlation between the two. Had we had more data points, we would have certainly found a more accurate correlation, but there were unfortunately so many strong emission lines to use from our spectrogram data.

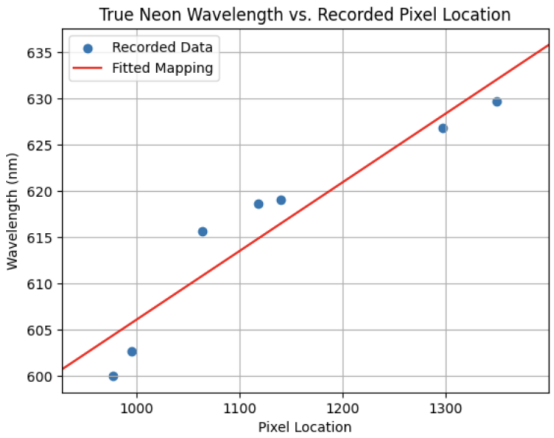

Figure 7: Polynomial Fit to True Neon Wavelength vs Recorded Pixel Location

2.3 Assessing Spectrograph Spatial Resolution and Wavelength Range

Simultaneous to the analysis performed above to convert pixel location to wavelength, we computed the spatial resolution of our spectrogram with the equations detailed in our introduction. Our wavelength range was from 651nm to 531nm - a middle value of 591nm returns a spectral resolution value of 177 at the center of the image. Aside from obtaining a wavelength range however, it was necessary to calculate the incidence angle θ_I, taking into account the groove density of our diffractor (600 diffracting lines/mm). The calculation was enabled by the Grating equation.

$$\theta(\text{rad}) = d\left(\sin(\theta_i) + \sin(\theta_d)\right)$$

This then allowed for the calculation of the angle of dispersion θ_D at the image center. θ_I and θ_D represent the angle at which light enters the spectrograph, and the angle at which light is dispersed by the spectrograph, respectively. The following shows the values we obtained or calculated for each variable included in the spectral resolution equation:

$\{\theta_I$:20.97, θ_D:-0.19, l_s: $100\mu m$, f_1:$75mm\}$

3 Sunlight Spectra Observations

This section is essentially what the previous parts of the report have all led up to converge to: obtaining the spectra of the sun, as precisely as possible. The spectrograph is calibrated, a program has been created which can approximate the wavelength of any emission line given its pixel location, and the spatial resolution is ready to calculate for any wavelength needed for analysis.

3.1 Obtaining Sunlight Images

As in the previous sections when collecting spectra from the gases, we used our spectrogram to collect the spectral signature of a light source. This time however, whereas we were looking for strong peaks in light, which has been referred to thus far as strong "emission lines", we must now look for "absorption lines) in the Sun's spectral lines, which instead are located in the troughs of a spectral signature. The two graphs below represents the data collected, from both the Sun and a randomly chosen cloud in the sky. Figure 9 specifically shows the location of the absorption lines, as well as the patterns of their spectral signatures.

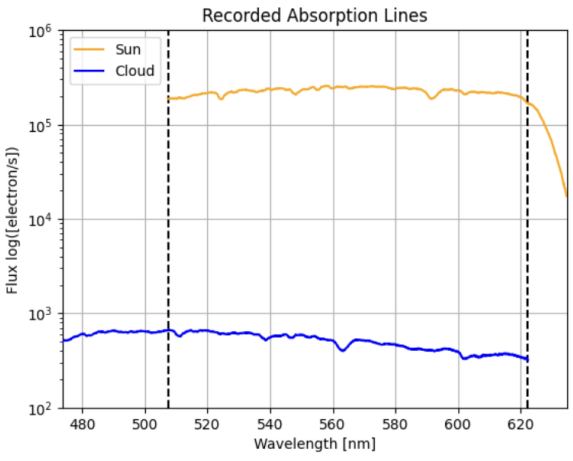

Figure 8: Recorded Absorption Lines Sun Cloud

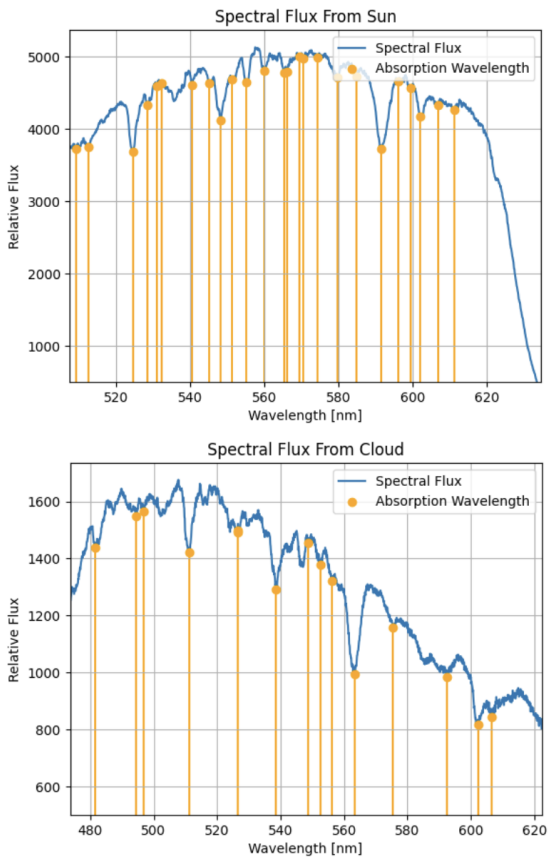

Figure 9: Spectral Flux from Sun Cloud

As can be expected, the flux, at any given wavelength, is evidently much higher (by a couple magnitudes) for the light taken in from the Sun versus a cloud. Also expected in the graphs, we can see the flux of the spectral signature from the Sun peak in the yellow range, and the cloud in the blue range. If one might recall from their kindergarten classes, it will come to mind that those are the corresponding colors of the objects (although the blue for the cloud comes from the air between the spectrograph and the cloud.) Now to add, we also see evident troughs in the graphed lines. We unfortunately cannot extrapolate the exact elements contained in their spectral signatures, since they are not comprised of one single element - it would thus be very difficult to differentiate the absorption lines correspond to specific elements.

3.2 Comparison of Flux Levels

It is however possible to compare the differences in the flux levels of the Sun and the cloud, which will allow us to approximate the slope of the power law between the two objects. With some quick plotting work, the graph below can be produced, plotting the ratio of the fluxes of the two objects, as they vary over a certain range of wavelengths.

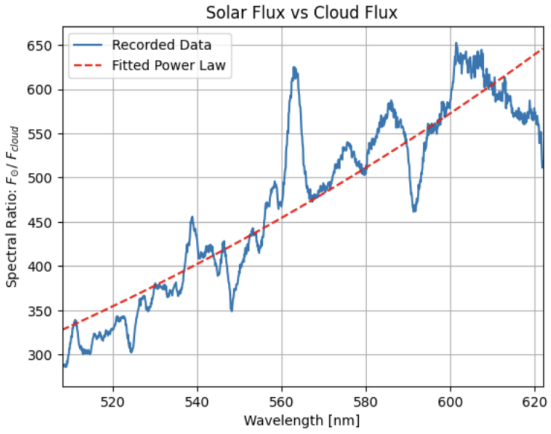

Figure 10: Solar Flux vs Cloud Flux

We characterize this slope at any given wavelength with the following equation:

$$\frac{F_{sky1}}{F_{sky2}} = \alpha\lambda^{\beta}$$

This helps us see how the flux of one object varies as a power of another, thus independent of the initial size of those quantities. It is necessary to do this due to the large difference in magnitudes between the two recorded fluxes.

4 Discussion/Conclusions

Evidently, there is a fair amount of precisional work to be done in obtaining the spectral signatures of bright objects or light sources. As previously mentioned, the spectrograph used in this lab had to be meticulously re-tuned to allow us to better view our strong emission lines. We came up with a couple of plotting/coding related solutions to help us approximate these strong lines better despite the blurriness of the images, caused by an incorrect angule of dispersion (not to be confused with angular dispersion, which is the angle at which the grooves of the diffractor are angled, not the diffractor itself). Once Professor Lu, of the UC Berkeley Department of Astronomy kindly re-aligned our spectrogram, we quickly took images of the Neon spectrum, and finished our analysis of its strongest emission lines to convert to wavelength, and finally get our wavelength range and spectral resolution. Given that all of our calibrating values (angle of incidence, disperson, slit width) were as expected, we continued on with our data collection, and compared the spectra of a Sun and a cloud in the sky. Their spectra came out as expected (yellower for the Sun, bluer for the cloud, as implied by the peaks in the spectral graphs), so we then looked at how they correlated according to the power law, and the fit was pleasantly linear, which confirmed, and concluded, the success of our experiment.

5 Acknowledgements

I would like to take the time to thank my lab partners, Cole Trudgen and Maxwell Coy, for their persistent efforts in this lab, making major efforts in sourcing the optimal Python libraries and modules to bring our lab results to fruition, along with other strong efforts in various other aspects of this lab. We were able to effectively coordinate our availabilities to spend as much time as possible working on this lab together, to ensure that our efforts were up to par with each other. I would also like to thank professors Jessica Lu and Alan Chew for their excellent advice and guidance throughout this lab, and the Astronomy Department at UC Berkeley for providing us with such an enriching lab experience. Finally, thank you to the reader of this report, I hope that I was able to concisely communicate and portray my lab results to you.

6 Appendix

6.1 Equations

Linear Least Squares Fitting

$$\hat{\beta} = \arg\min_{\beta} \left(\sum_{i=1}^{n} \frac{(y_i - p(x_i, \beta))^2}{\sigma_i^2} \right)$$

- $\hat{\beta}$: Estimated coefficients of the polynomial.
- y_i: Observed value at point i.
- $p(x_i, \beta)$: Polynomial model evaluated at x_i with coefficients β.
- σ_i^2: Variance of the observation at i (if errors have different variances; omit if errors are uniform).
- n: Number of data points.

Wavelength Range

$$\Delta\lambda = \lambda_{\text{sl, max}} - \lambda_{\text{sl, min}}$$

Spectral Resolution

$$R = 1000 \left(\frac{f_1 \left(\sin(\text{radians}(\theta_I)) + \sin(\text{radians}(\theta_D)) \right)}{l_s \cos(\text{radians}(\theta_D))} \right)$$

- f_1: Focal length (in mm) of optical lens.
- θ_I: Angle of incidence, the angle at which light enters the spectrograph.
- θ_D: Angle of dispersion, the angle at which light is dispersed by the spectrograph.
- l_s: Width of the slit through which light enters the spectrograph.

Final Frame Cleaning

$$\textbf{Cleaned Frame} = \frac{S - D_S}{norm\,(F - D_F)}$$

Variables (all in ADU [Noise Level])

- S : Spectral Frame
- F : Flat Frame
- D_S : Dark Frame from Spectral Frame
- D_F : Dark Frame from Flat Frame (Equal to D_S)

6.2 Python Libraries

- matplotlib.pyplot
- numpy
- readData
- from scipy.signal (find_peaks)

7 References

- [1] “Strong Lines of Neon (Ne).” Basic Atomic Spectroscopic Data, National Institute of Standards and Technology, Physical Measurement Laboratory, physics.nist.gov/PhysRefData/Handbook/Tables/neontable2.htm. Accessed 8 Oct. 2024.